

Investigation of the effect of variable layer thickness on PLA parts produced with FDM 3D printer

Vedat Taşdemir*

Department of Mechanical Engineering, Simav Technology Faculty, Kütahya Dumlupınar University, 43500 Kütahya, Türkiye

*Corresponding Author's Tel: +90-(274)-443-50-04, E-mail address: vedat.tasdemir@dpu.edu.tr
ORCID: 0000-0002-2375-9525

Abstract

The study experimentally investigated the effects of using 0.1, 0.2, and 0.3 mm layer thicknesses determined within the same structure on tensile strength and build time. The tensile test sample thickness (3.6 mm) was divided into three sheets with different layer thicknesses, and the effect of the ratio of the inner sheet thickness (1.2 mm, 1.8 mm, and 2.4 mm) to the sample thickness was also evaluated. The experimental results were also analyzed using the Pareto front multi-objective optimization method. While the lowest tensile strengths were obtained in samples where 0.2 mm and 0.3 mm layer thicknesses were used together, the highest tensile strengths were obtained in samples where 0.1 mm layer thickness was used together with 0.2 mm and 0.3 mm layers. Significant savings were achieved considering the production times of samples with fixed and variable layer thicknesses. When tensile strength and build time are optimized, optimum results for the most balanced solution were obtained using 0.3 mm outer sheet layer thicknesses and 0.1 mm inner sheet layer thicknesses. This situation also directly affects production costs. As a result of the study, it was determined that variable layer thickness is significant in terms of both strength and build time.

Keywords: Additive manufacturing, 3D printing, FDM, variable layer thickness, PLA, Pareto front

1. Introduction

Also known as additive manufacturing or rapid prototyping, 3D printing is gaining more and more attention over traditional (subtractive) methods due to both environmental impact and processing advantages [1–3]. In this technology, materials are combined in layers to obtain three-dimensional

objects. Rapid developments in additive manufacturing technology have increased use in the biomedical [4], aviation, military [5], automotive, maritime, food, clothing, architecture and electronic industries [6, 7]. Especially the minimum material loss, absence of geometric limitations, and low production costs have caused the rapid development of 3D printing technology [8, 9].

Today, widely used stereolithography (SLA), fused filament fabrication (FFF)/fused deposition modeling (FDM), laminated object manufacturing (LOM), selective laser sintering (SLS), selective laser melting (SLM), electron beam melting (EBM), PolyJet (PJ) and direct metal laser sintering (DMLS), etc. there are many additive manufacturing technologies [10]. In addition to existing technologies, many new technologies are being introduced in the market depending on the developing conditions of the day. One of the most popular of these technologies is Fused Deposition Modeling (FDM). This technology is widely used, especially in producing polymer and composite components [11–13].

Since additive manufacturing is solid free-form technology and allows great design freedom, its use is increasing in every field. Generally, products with smooth surfaces very close to the desired dimensions can be produced using the most commercially available 3D printers [14, 15]. However, printing parameters need to be well-known and evaluated to make quality objects [16]. There are many parameters commonly used to determine the mechanical properties of samples obtained through the FDM/FFF process. As a result of the examination, the most important parameters are, layer height/thickness, structure direction [17], nozzle temperature fill density [18], number of shells [19], raster direction, spacing between raster and raster width can be said [20, 21]. Anisotropic behaviour plays an important role in manufactured parts, as process parameters can vary [22].

The dimensional integrity of the products produced is directly related to the layer thickness. Dimensional accuracy is closer to what is desired when small layer thicknesses are used, but in this case, the build time is considerably increased. On the other hand, when large layer thicknesses are used, the build time is reduced, but also, in this case, the dimensional accuracy is reduced [23]. However, there are some cases where reducing the layer thickness does not reduce errors [24]. In particular, the use of variable additive manufacturing will be more effective in terms of dimensional completeness than the construction of curved surface structures [25]. In addition, the mechanical properties of samples with low layer thicknesses are relatively higher than those of samples with high layer thicknesses [26, 27].

There are many studies in the literature examining the effect of production parameters on the mechanical properties of the parts produced with 3D printers. When these parameters used for the production of the parts are examined, they are seen as constant throughout the production. One of the most frequently used parameters among these parameters is layer thickness. In this study, variable layer thicknesses were used in the same structure. In this respect, it can be said that the study is original and will make a scientific contribution. The study aims to examine the effect of different layer thicknesses used in the same structure.

There are many studies in the literature that examine the effects of different production parameters on the mechanical properties of parts produced with FDM 3D printers. When the various parameters used in the production of parts are discussed, it is seen that the parameters used throughout the production of the part are kept constant. One of the most frequently used parameters among these parameters is the layer thickness. When the studies were examined, no studies were found on using variable layer thicknesses in the same structure and their effect on mechanical properties. Unlike the literature, this study was carried out using variable layer thicknesses in the same structure. In this respect, it can be clearly said that the study is original and will make a scientific contribution. The aim of the study is to examine the effect of different layer thicknesses used in the same structure.

2. Material and Method

PLA is one of the most popular thermoplastics for FDM-type 3D printers [28, 29]. This bioplastic is made from renewable resources such as corn, beets, or potatoes. PLA is an environmentally friendly bio-polymer compared to petroleum-based plastic materials such as ABS, polyethylene, and polypropylene [30, 31]. Flashforge Creator 3 Pro FDM 3D printers with an independent double extruder were used in the production of the tensile samples. The study was carried out using PLA (Polylactic Acid) thermoplastic. When the studies are examined, the layer thicknesses mainly vary between 0.1 mm and 0.3 mm. In this study, the layer thickness selection was made by considering the commonly used layer thicknesses. Samples were produced using variable layer thicknesses (0.1, 0.2, 0.3) and layer thickness ratios (33.33 %, 50 %, 66.66 %, and 100 %) within the same structure. The study used six variable layer thickness design levels and three different inner sheet ratio levels. The experiment design (DOE) was made as full factorial according to these two factors (variable layer thickness design and inner sheet ratio) and their levels and is presented in Table 2.

The experimentally obtained results were presented with the best solution using the Pareto front multi-objective optimization technique. The production scheme of samples and an image of the manufactured product with variable layer thickness is shown in Figure 1. 3D printing processes were carried out using the experimental parameters given in Table 1. Tensile test specimens were manufactured with different layer thicknesses, as seen in Figure 2. Tensile specimens were produced according to ASTM D638-Type IV standard and with a thickness of $t = 3.6$ mm (Figure 2). Tensile tests were carried out on a Zwick/Roell Z100 testing machine at a speed of 1 mm.s^{-1} (Figure 3).

Figure 1

In Figure 1, n_1 and n_2 are the outer and inner layer numbers, f_1 and f_2 are the outer and inner sheet layer thicknesses, t_1 and t_2 are the outer and inner sheet thicknesses, and t is the total thickness of the tensile test sample. In the study, outer layer thicknesses were kept the same on both sides. The most important reason for keeping the outer layer thicknesses the same on both sides is to fully determine the effect of the change in inner sheet layer thickness and inner sheet layer thickness ratio.

Figure 2

Table 1

Figure 3

Table 2

In this study, we have two goals. Our first goal is to maximize the tensile strength (the higher value is better). Our second goal is to minimize the construction time (the lower value is better). In this context, a mathematical approach based on the dominance relationship was used to determine the Pareto optimal set. The dominance relationship (Pareto Dominance) is defined by the mathematical functions given in Equation 1 and Equation 2 [32].

Minimize:

$$\forall i \in \{1, 2, \dots, k\} : f_i(x^*) \leq f_i(x) \text{ and } \exists j \in \{1, 2, \dots, k\} : f_j(x^*) < f_j(x) \quad (1)$$

Maximize:

$$\forall i \in \{1, 2, \dots, k\} : f_i(x^*) \geq f_i(x) \text{ and } \exists j \in \{1, 2, \dots, k\} : f_j(x^*) > f_j(x) \quad (2)$$

Here, $f_i(x)$: the value of the i . objective function, k : the total number of objectives, x^* and x : the two solutions being compared. In this function, x^* performs at least equally to x in all objectives,

and x^* is definitely better than x in at least one objective. This formula is the cornerstone of multi-objective optimization. When applied correctly, it helps us determine the most efficient solutions.

3. Results and Discussions

The variable layer thickness process allows us to divide the products desired to be produced into one or more areas. A design with thicker or thinner layers can be created depending on the model's intended use. If there is a section that does not contain much detail about the product to be produced, we can print that section with a thicker layer to save time. However, if there is a section with details, it should be printed with a thinner layer to reveal the details and increase the print quality. The use of both thin and thick layer thicknesses while producing the products provides significant contributions in terms of build time and production cost.

The highest tensile strength was obtained with 50,677 MPa in Experiment 19 (Figure 4). The layer thickness of this sample was kept constant at 0.1 mm, and the build time was 48 minutes. When we compare sample number 19, which has the highest tensile strength, with the samples produced using variable layer thickness, it is clearly seen that although there is no significant change in tensile strength, the build time is very long. This shows how important variable layer thickness is in saving build time and cost. All samples produced for the study were produced with a 100 % infill density. The rates of 33.33 %, 50 %, and 66.66 % in the tests express the ratio of the inner sheet thickness (t_2) to the sample thickness (t) on the inside. When the tensile test results of the samples with different layer thicknesses were examined, the best result for all ratios was obtained in the structure "0.3 x 0.1 x 0.3". The tensile strength of Sample 19 was 1.68% higher than Sample 5, 0.7 % higher than Sample 11, and 0.61 % higher than Sample 17. In this case, it can be said that the change is not very important. Again, the tensile strength of Sample 19 was 4.86 % and 5.62 % greater than the tensile strength of Samples 20 and 21, respectively. All of the samples with the smallest tensile strength were obtained in combinations of 0.2 mm and 0.3 mm layer thicknesses.

Considering the build times of the samples, the build time, which was 48 minutes for Sample 19, decreased to 31, 36, and 39 minutes for Samples 5, 11, and 17, respectively. Although Samples 5, 11, and 17 are all produced in the structure of "0.3 x 0.1 x 0.3", the build times vary depending on the increase in the thickness of the inner sheet thickness. Considering the build times, the build time of Sample 19 (with a constant layer thickness of 0.1 mm) was found to be 54.8 %, 37.1 %, and 23 % longer, respectively, than the build time of Samples 5, 11, and 17 with variable layer

thickness (Figure 5). This results in a significant increase in cost and time lost. It can also be said that the effect of the increase in the inner sheet thickness ratio (t_2/t) on the tensile strength is minimal. In addition, as the inner sheet thickness (t_2) increases, it has been observed that the build time changes significantly depending on the layer thickness (Figure 6).

Figure 4

Figure 5

Figure 6

When there is more than one objective or criterion in a system, it is necessary to determine how to achieve the most optimal balance between these objectives [33]. In such multi-objective optimization problems, the Pareto front can play an essential role in providing the best solutions. Multi-objective optimization (MOO) problems are applied to complex systems where there are multiple objective functions that conflict with each other and usually cannot be optimized simultaneously. In such problems, instead of a single global optimum, there is a set of Pareto-optimal solutions that represent trade-offs between the objectives. Mathematically, a solution is considered Pareto-optimal if and only if the value of no objective function can be improved without worsening the values of the other objective functions. The geometric projection of these solutions on the objective function space is called the Pareto frontier and can generally exhibit convex, non-convex, or disconnected structures. MOO optimization approaches offer decision-makers optimal solution alternatives in a wide range of applications, from engineering design to financial planning. When the data in Table 2 was analyzed with the Pareto front, the graph in Figure 7 was obtained. Figure 7 presents a situation where the strength is maximized and the production time is minimized. For the Pareto optimal set, samples numbered 5, 6, 15, 17 and 19 given in Table 3 were determined, and the red line connecting these points shows the Pareto front. When the graph is examined, sample 5 offers the most balanced solution. Again, when the graph is examined, sample 6 has the fastest production time but the lowest strength. However, sample 19 is the sample with the highest strength and the slowest in terms of production time. It can be said that the area between sample 5 and sample 6 is the most critical area for the time-strength balance. Here, it is seen that sample 5 offers the most balanced solution. When samples 5 and 6 are compared, if strength is to be accepted as a criterion, this trade-off can be accepted. Again, when comparing sample number 5 with sample number 19, the strength increase of sample number 19 (+0.841 MPa) provides a minimal gain that is not worth the time increase (+17 min). In summary, sample number 6 should be preferred for

fast production (if time is a priority), sample number 5 for balanced performance (if both time and strength are essential) and sample number 17 for high strength (if maximum strength is required).

Figure 7

Table 3

Small layer thicknesses caused the gaps between layers to decrease, resulting in higher tensile strength (Figure 8). On the other hand, small layer thicknesses cause high build time and cost increases (Table 2). Despite the same tensile strength, the study shows how important variable layer thickness is in terms of lower build time and cost.

Figure 8

The modulus of elasticity expresses the rigidity, that is, the resistance of a material to elastic deformation. A high modulus of elasticity means that the material is rigid or that the elastic strain resulting from applied stress will be minor; for the samples produced with fixed layer thickness, the highest modulus of elasticity was obtained with 3.058 GPa in Sample 21 with a layer thickness of 0.3 mm. In samples with variable layer thickness, the highest modulus of elasticity (3.235 GPa) was obtained in Sample 10 with a combination of “0.2 x 0.3 x 0.2” layer thickness. This shows that higher layer thicknesses are more rigid and more resistant to elastic deformation.

In addition, it has been observed that the variable layer thickness adversely affects the dimensional accuracy of flat-form parts. When the dimensions of tensile specimens with variable layer thickness are measured, deviations of up to 0.15 mm have also been found (Figure 9). It was observed that the most significant deviation values were in the samples where 0.1 mm and 0.3 mm layers were used together. This shows that the use of variable layer thickness on curved and inclined parts is much more important in terms of dimensional accuracy than on prismatic-shaped parts with vertical surfaces. Gohari et al. [34] stated that the use of the adaptive variable layer thickness method reduced the number of layers needed by 25 %, and also reduced geometric errors and surface roughness compared to the part produced using minimum layer thickness.

Figure 9

Figure 10

The highest elongation was observed in samples with an inner layer thickness (f_2) of 0.1 mm, and the lowest elongation was observed in samples with an inner layer thickness (f_2) of 0.3 mm (Figure 10). Accordingly, the lowest elongation was obtained in Sample 10, which has a structure of “0.2 x 0.3 x 0.2” with 3.26 %, and the highest elongation was obtained in Sample 11, with a structure

of “0.3 x 0.1 x 0.3” with 10.18%. When the tests are examined, as the inner sheet thickness (t_2) increases, the elongation also increases. In Sample 19 (0.1 mm), Sample 20 (0.2 mm), and Sample 21 (0.3 mm) with fixed layer thickness, the elongation was 5.35 %, 5.48 %, and 5.71 %, respectively.

4. Conclusions

The study investigated the effect of using different layer thicknesses in the same structure on both mechanics and build time. The samples obtained within the scope of the study were produced with FDM 3D printing. The lowest tensile strength was obtained in the experiments where 0.2 mm and 0.3 mm layer thicknesses were used together, and the highest tensile strengths were obtained in the samples where 0.1 mm layer thickness was used together with 0.2 and 0.3 mm layers. As the layer thickness decreases, the gap decreases, which increases the tensile strength. From the MOO analysis, it was determined that sample number 6 could be preferred for fast production (if time is a priority), sample number 5 could be selected for balanced performance (if both time and strength are essential), and sample number 17 could be preferred for high strength (if maximum strength is required). When the results were optimized for the most balanced solution, the optimum result was obtained: the outer sheet layer thickness was 0.3 mm, the inner sheet layer thickness was 0.1 mm, and the inner sheet thickness ratio was 33.33%. The inner sheet thickness (t_2) ratio increase did not significantly change the tensile strength but significantly affected the printing time. Higher layer thicknesses gave better results in terms of the modulus of elasticity. When the samples produced with constant layer thickness are compared with the samples made with variable layer thickness, although there is no significant difference in terms of tensile strength, there is a very big difference in terms of build time. The operation can be further expanded by using different fill rates, different printing speeds, different production temperatures, different orientation angles, and different types of materials. It can also be used especially for the production of porous structures.

Funding

Not applicable

Conflicts of interest/Competing interests

The authors declare that they have no conflict of interest.

Availability of data and material

Not applicable (The authors affirm that the data supporting the results of this study and the used equipment are available within the article.)

Code availability

Not applicable

Ethics approval

Not applicable

Consent to participate

Not applicable

Consent for publication

Not applicable

Authors' contributions

All authors contributed to the study's conception.

References

- [1] Dobos, J., Hanon, M.M., Oldal, I., “Effect of infill density and pattern on the specific load capacity of FDM 3D-printed PLA multi-layer sandwich.” *J. Polym. Eng.* 42:118–128:(2022). <https://doi.org/10.1515/polymeng-2021-0223>
- [2] Frazier, W.E., “Metal additive manufacturing: A review.” *J. Mater. Eng. Perform.* 23:1917–1928:(2014). <https://doi.org/10.1007/s11665-014-0958-z>
- [3] Yermurat, B., Seçgin, Ö., Taşdemir, V., “Multi-material additive manufacturing : investigation of the combined use of ABS and PLA in the same structure.” *Mater. Test.* 65:1119–1126:(2023). <https://doi.org/10.1515/mt-2022-0368>
- [4] Kamer, M.S., Temiz, Ş., Yaykaşlı, H., et al., “Comparison of mechanical properties of tensile test specimens produced with ABS and PLA material at different printing speeds in 3D printer.” *J. Fac. Eng. Archit. Gazi Univ.* 37:1197–1211:(2022). <https://doi.org/10.17341/gazimmfd.961981>
- [5] Seçgin, Ö., Arda, E., Ata, E., et al., “Dimensional optimization of additive manufacturing process.” *J. Chinese Soc. Mech. Eng.* 43:75–78:(2022). <https://doi.org/https://doi.org/10.29979/JCSME>
- [6] Gonabadi, H., Chen, Y., Yadav, A., et al., “Investigation of the effect of raster angle, build orientation, and infill density on the elastic response of 3D printed parts using finite

- element microstructural modeling and homogenization techniques.” *Int. J. Adv. Manuf. Technol.* 118:1485–1510:(2022). <https://doi.org/10.1007/s00170-021-07940-4>
- [7] Andrzejewska, A.J., “Experimental study on the effect of selected sterilization methods on mechanical properties of polylactide FFF specimens.” *Rapid Prototyp. J.* 29:1–6:(2022). <https://doi.org/10.1108/RPJ-05-2021-0115>
- [8] Yu, W., Shi, J., Sun, L., et al., “Effects of printing parameters on properties of FDM 3D printed residue of astragalus/polylactic acid biomass composites.” *Molecules* 27:(2022). <https://doi.org/10.3390/molecules27217373>
- [9] Yao, T., Ye, J., Deng, Z., et al., “Tensile failure strength and separation angle of FDM 3D printing PLA material: Experimental and theoretical analyses.” *Compos. Part B Eng.* 188:107894:(2020). <https://doi.org/10.1016/j.compositesb.2020.107894>
- [10] Zhang, Q., Cai, H., Zhang, A., et al., “Effects of lubricant and toughening agent on the fluidity and toughness of poplar powder-reinforced polylactic acid 3D printing materials.” *Polymers (Basel)*. 10:(2018). <https://doi.org/10.3390/polym10090932>
- [11] Dudek, P., “FDM 3D printing technology in manufacturing composite elements.” *Arch. Metall. Mater.* 58:1415–1418:(2013). <https://doi.org/10.2478/amm-2013-0186>
- [12] Vijayakumar, M.D., Palaniyappan, S., Veeman, D., et al., “Process optimization of hexagonally structured polyethylene terephthalate glycol and carbon fiber composite with added shell walls.” *J Mater Eng Perform.* <https://doi.org/10.1007/s11665-022-07572-z>
- [13] Taşcıoğlu, E., Kıtay, Ö., Keskin, A.Ö., et al., “Effect of printing parameters and post-process on surface roughness and dimensional deviation of PLA parts fabricated by extrusion-based 3D printing.” *J. Brazilian Soc. Mech. Sci. Eng.* 44:1–14:(2022). <https://doi.org/10.1007/s40430-022-03429-7>
- [14] Abeykoon, C., Sri-Amphorn, P., Fernando, A., “Optimization of fused deposition modeling parameters for improved PLA and ABS 3D printed structures.” *Int. J. Light. Mater. Manuf.* 3:284–297:(2020). <https://doi.org/10.1016/j.ijlmm.2020.03.003>
- [15] Zonoobi, M.A., Haghshenas Gorgani, H., Javaherneshan, D., “Experimental investigation and multi-objective optimization of FDM process parameters for mechanical strength, dimensional accuracy, and cost using a hybrid algorithm.” *Sci. Iran.* 0:0–0:(2023). <https://doi.org/10.24200/sci.2023.60960.7090>
- [16] Sepahi, M.T., Abusalma, H., Jovanovic, V., et al., “Mechanical properties of 3D-printed

- parts made of polyethylene terephthalate glycol.” *J. Mater. Eng. Perform.* 30:6851–6861:(2021). <https://doi.org/10.1007/s11665-021-06032-4>
- [17] Auffray, L., Gouge, P.A., Hattali, L., “Design of experiment analysis on tensile properties of PLA samples produced by fused filament fabrication.” *Int. J. Adv. Manuf. Technol.* 118:4123–4137:(2022). <https://doi.org/10.1007/s00170-021-08216-7>
- [18] Vogel, D., Weißmann, V., Rührmund, L., et al., “Influence of nozzle temperature and volumetric filling on the mechanical properties of 3D-printed PEEK.” *Mater. Test.* 62:351–356:(2020). <https://doi.org/10.3139/120.111490>
- [19] Olam, M., Tosun, N., “Assessment of 3D printings produced in fused deposition modeling printer using polylactic acid/TiO₂/hydroxyapatite composite filaments.” *J. Mater. Eng. Perform.* 31:4554–4565:(2022). <https://doi.org/10.1007/s11665-021-06539-w>
- [20] Roj, R., Blondrath, A., Theiß, R., et al., “Quality optimization of FDM-printed (fused deposition modeling) components based on differential scanning calorimetry.” *Mater. Test.* 64:1544–1551:(2022). <https://doi.org/10.1515/mt-2022-0199>
- [21] Taşdemir, V., “Investigation of the effects of the number of shells, raster angle, extrusion ratio, and path width on printed polylactic acid parts with fused deposition modeling 3D printer.” *J. Mater. Eng. Perform.* 33:11888–11898:(2024). <https://doi.org/10.1007/s11665-024-09863-z>
- [22] Algarni, M., Sami, G., “Comparative study of the sensitivity of PLA, ABS, PEEK, and PETG’s mechanical properties to FDM printing process parameters.” *crystals* 11:995:(2021). <https://doi.org/10.1016/b978-075065129-5/50007-6>
- [23] Taşdemir, V., “Investigation of dimensional integrity and surface quality of different thin-walled geometric parts produced via fused deposition modeling 3D printing.” *J. Mater. Eng. Perform.* 30:3381–3387:(2021). <https://doi.org/10.1007/s11665-021-05809-x>
- [24] Gohari, H., Barari, A., Kishawy, H., et al., “Intelligent process planning for additive manufacturing.” *IFAC-PapersOnLine* 52:218–223:(2019). <https://doi.org/10.1016/j.ifacol.2019.10.067>
- [25] Shah, J., Snider, B., Clarke, T., et al., “Large-scale 3D printers for additive manufacturing: design considerations and challenges.” *Int. J. Adv. Manuf. Technol.* 104:3679–3693:(2019). <https://doi.org/10.1007/s00170-019-04074-6>
- [26] Wang, C.C., Lin, T.W., Hu, S.S., “Optimizing the rapid prototyping process by integrating

- the Taguchi method with the gray relational analysis.” *Rapid Prototyp. J.* 13:304–315:(2007). <https://doi.org/10.1108/13552540710824814>
- [27] Zhao, Y., Chen, Y., Zhou, Y., “Novel mechanical models of tensile strength and elastic property of FDM AM PLA materials: Experimental and theoretical analyses.” *Mater. Des.* 181:1–10:(2019). <https://doi.org/10.1016/j.matdes.2019.108089>
- [28] Torun, A.R., Dike, A.S., Yıldız, E.C., et al., “Fracture characterization and modeling of gyroid filled 3D printed PLA structures.” *Mater. Test.* 63:397–401:(2021). <https://doi.org/10.1515/mt-2020-0068>
- [29] Eryildiz, M., “Comparison of notch fabrication methods on the impact strength of FDM-3D-printed PLA specimens.” *Mater. Test.* 65:423–430:(2023). <https://doi.org/10.1515/mt-2022-0306>
- [30] Ayrimis, N., “Effect of layer thickness on surface properties of 3D printed materials produced from wood flour/PLA filament.” *Polym. Test.* 71:163–166:(2018). <https://doi.org/10.1016/j.polymertesting.2018.09.009>
- [31] Mathiazhagan, N., Palaniyappan, S., Sivakumar, N. kumar., “Effect of fused filament fabrication parameters on crashworthiness studies of hydroxyapatite particle reinforced PLA composite thin-walled tubes.” *J. Mech. Behav. Biomed. Mater.* 138:105611:(2023). <https://doi.org/10.1016/j.jmbbm.2022.105611>
- [32] Kang, S., Li, K., Wang, R., “A survey on pareto front learning for multi-objective optimization.” *J Membr Comput.* <https://doi.org/10.1007/s41965-024-00170-z>
- [33] Kalyanmoy, D., “Multi-objective optimization.” In: Burke EK, Graham K (eds) Search methodologies: Introductory tutorials in optimization and decision support techniques, 2nd ed., pp 403–449, Springer, Boston, MA (2014). https://doi.org/10.1007/978-1-4614-6940-7_15
- [34] Gohari, H., Kishawy, H., Barari, A., “Adaptive variable layer thickness and perimetral offset planning for layer-based additive manufacturing processes.” *Int. J. Comput. Integr. Manuf.* 34:964–974:(2021). <https://doi.org/10.1080/0951192X.2021.1946854>

Figure Captions

Figure 1. Variable layer thickness, a) Schematic representation, b) Image of the manufactured product

Figure 2. Tensile test sample with variable layer thickness (0.3 x 0.1 x 0.3)

Figure 3. View before and after the tensile test (for Sample 7)

Figure 4. Comparison of tensile test results

Figure 5. Effect of change of inner sheet thickness ratio a) Tensile strength b) Build time (The ratios are Sample 5, 11, 17, and 19, respectively)

Figure 6. Effect of change of inner layer thickness a) Tensile strength b) Build time (Layer thicknesses are Samples 3, 20, and 4, respectively)

Figure 7. Pareto front in multi objective optimization

Figure 8. The gap between the layers depending on the layer thickness

Figure 9. Sample produced according to variable layer thickness

Figure 10. The stress-strain graph of test samples

Table Captions

Table 1. Parameters used for a 3D printer

Table 2. Experiment design and results

Table 3. Pareto-optimal set

Figures

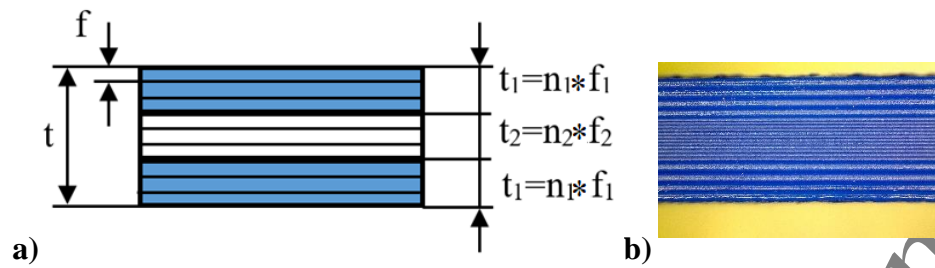


Figure 1. Variable layer thickness, a) Schematic representation, b) Image of the manufactured product

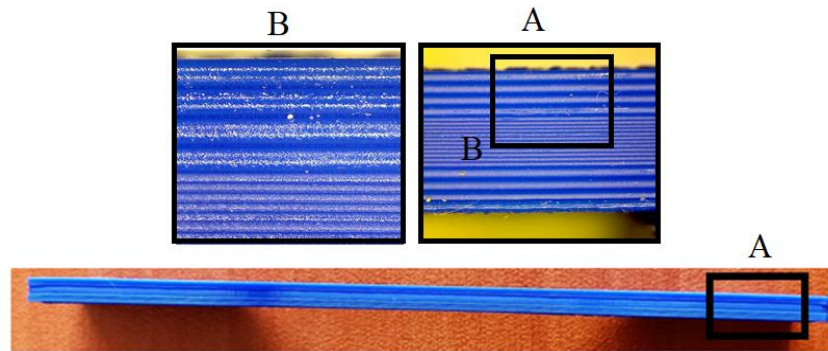


Figure 2. Tensile test sample with variable layer thickness (0.3 x 0.1 x 0.3)

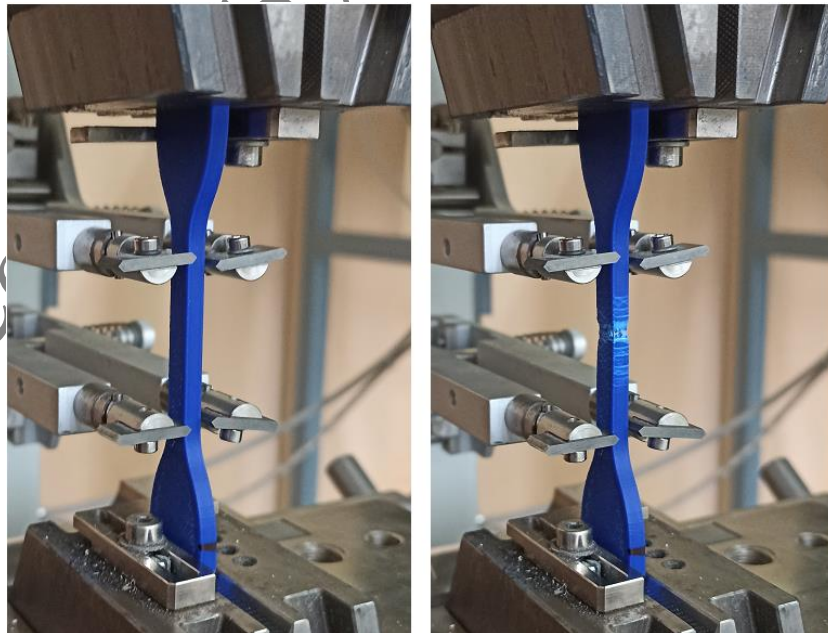


Figure 3. View before and after the tensile test (for Sample 7)

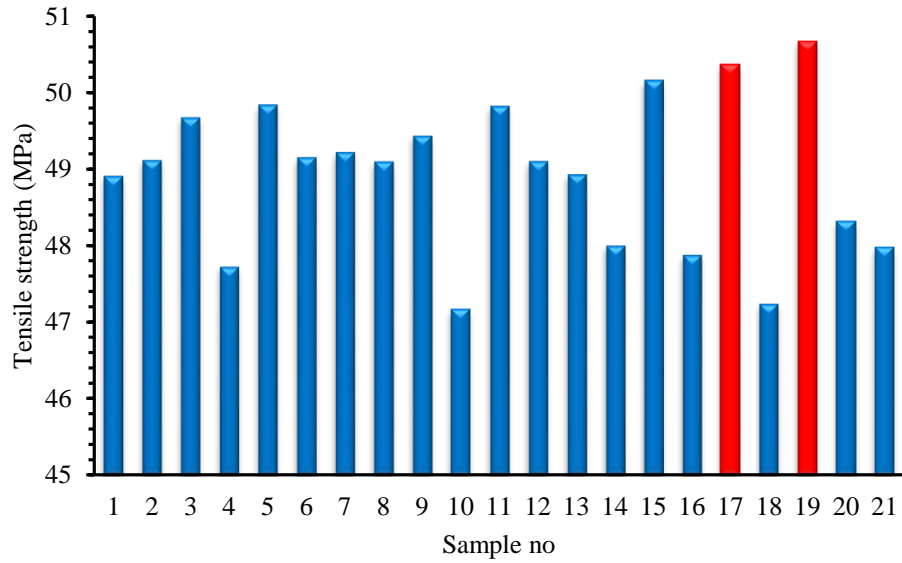
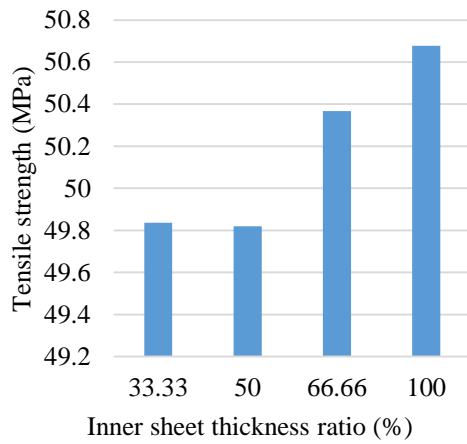
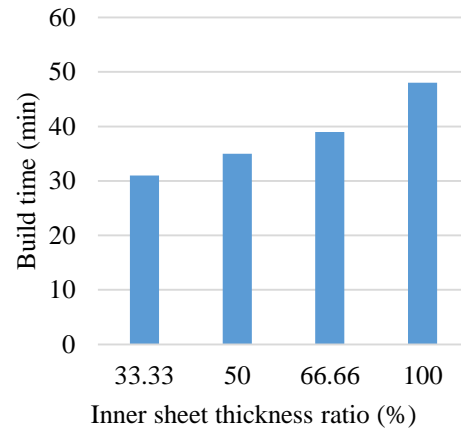


Figure 4. Comparison of tensile test results



a)



b)

Figure 5. Effect of change of inner sheet thickness ratio a) Tensile strength b) Build time (The ratios are Sample 5, 11, 17, and 19, respectively)

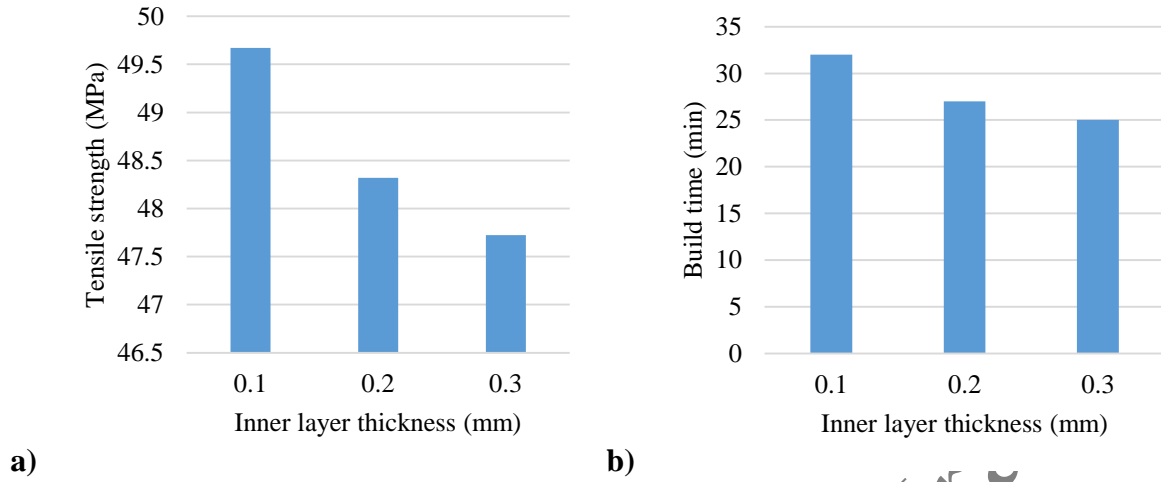


Figure 6. Effect of change of inner layer thickness a) Tensile strength b) Build time (Layer thicknesses are Samples 3, 20, and 4, respectively)

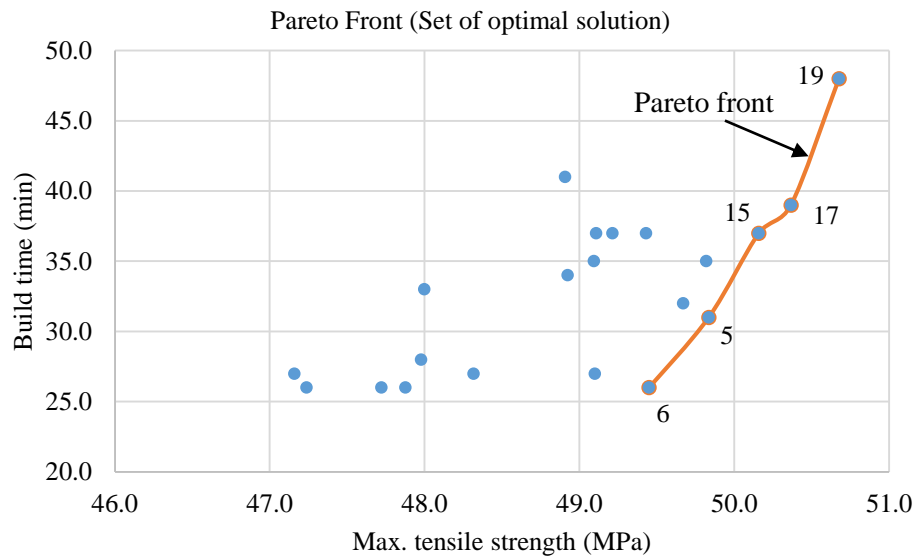


Figure 7. Pareto front in multi objective optimization

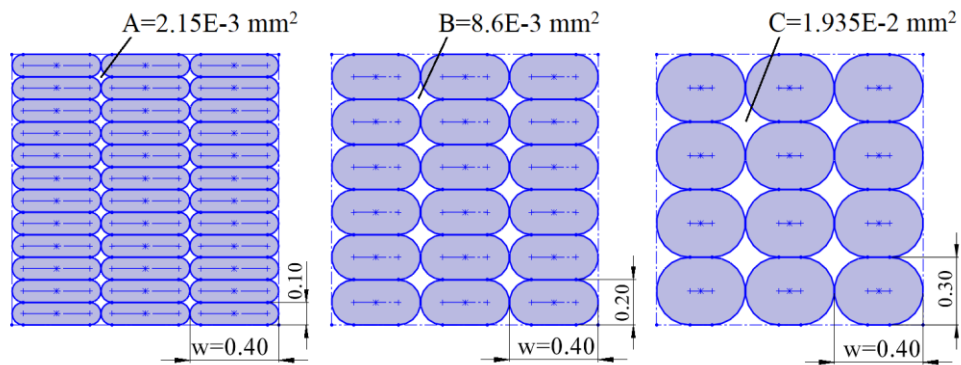


Figure 8. The gap between the layers depending on the layer thickness

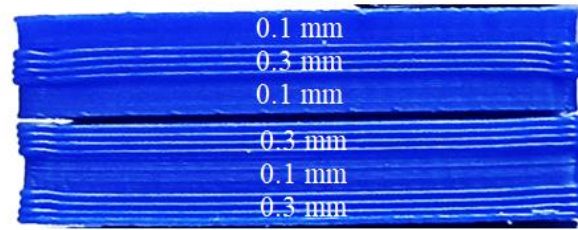


Figure 9. Sample produced according to variable layer thickness

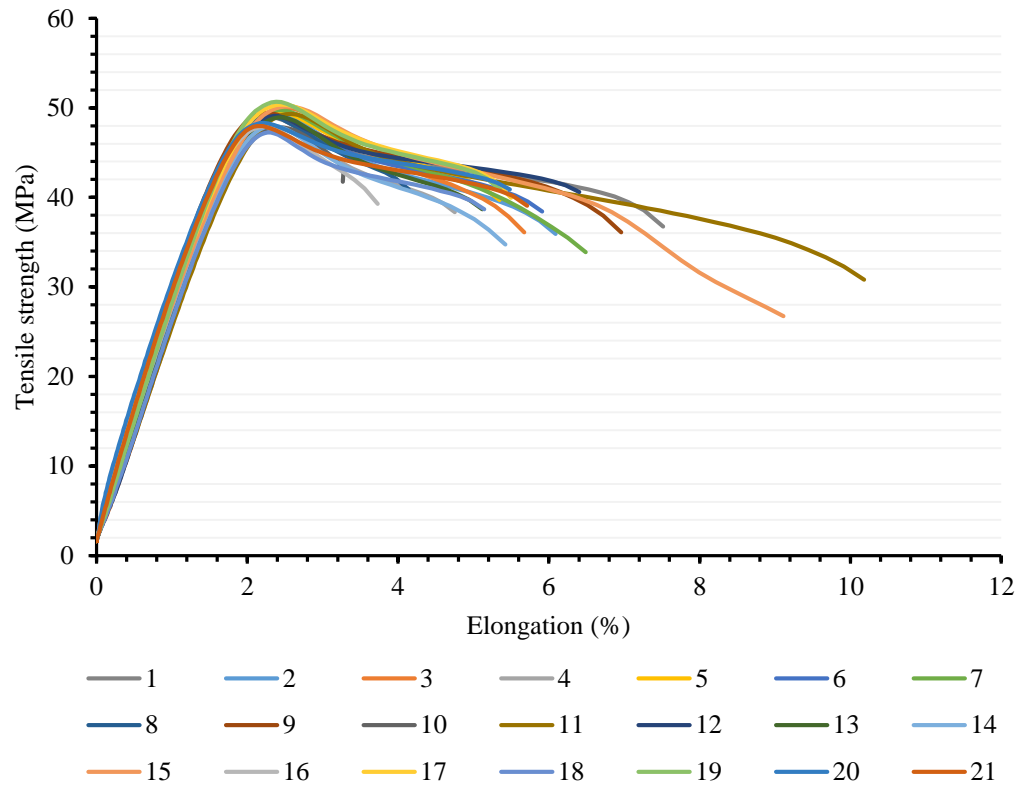


Figure 10. The stress-strain graph of test samples

Tables

Table 1. Parameters used for a 3D printer

| Properties | Value |
|---|--------------------------|
| Material | PLA |
| Density (g.cm ⁻³) | 1.2 |
| Nozzle temperature (°C) | 205 |
| Bed temperature (°C) | 45 |
| Nozzle diameter (mm) | 0.4 |
| Filament diameter (mm) | 1.75 ±0.05 |
| Wall thickness (mm) | 1.2 |
| Infill density (%) | 100 |
| Layer height (f) (mm) | Variable (0.1, 0.2, 0.3) |
| Number of upper solid layers | 0 |
| Number of subfloor layers | 0 |
| Path width (w) (mm) | 0.4 mm |
| Inner sheet thickness ratio (t ₂ /t) (%) | 33.33, 50, 66.66 |
| Basic print speed (mm.s ⁻¹) | 60 |

Table 2. Experiment design and results

| S. No | Infill density | Inner sheet thickness ratio (t ₂ /t) | t ₁ × t ₂ × t ₁ (mm) | Outer sheet layer thickness (f ₁) (mm) | Inner sheet layer thickness (f ₂) (mm) | Outer sheet layer thickness (f ₁) (mm) | Max. tensile strength (MPa) | Young's modulus (GPa) | Build time (min) |
|-------|----------------|---|---|--|--|--|-----------------------------|-----------------------|------------------|
| 1 | 100 % | 33.33 % | 1.2 × 1.2 × 1.2 | 0.1 | 0.2 | 0.1 | 48.908 | 2.555 | 41 |
| 2 | | | | 0.1 | 0.3 | 0.1 | 49.110 | 2.532 | 37 |
| 3 | | | | 0.2 | 0.1 | 0.2 | 49.671 | 2.535 | 32 |
| 4 | | | | 0.2 | 0.3 | 0.2 | 47.722 | 2.534 | 26 |
| 5 | | | | 0.3 | 0.1 | 0.3 | 49.836 | 2.617 | 31 |
| 6 | | | | 0.3 | 0.2 | 0.3 | 49.150 | 2.667 | 26 |
| 7 | 100 % | 50 % | 0.9 × 1.8 × 0.9 | 0.1 | 0.2 | 0.1 | 49.215 | 3.116 | 37 |
| 8 | | | | 0.1 | 0.3 | 0.1 | 49.094 | 2.833 | 35 |
| 9 | | | | 0.2 | 0.1 | 0.2 | 49.431 | 3.129 | 37 |
| 10 | | | | 0.2 | 0.3 | 0.2 | 47.161 | 3.235 | 27 |
| 11 | | | | 0.3 | 0.1 | 0.3 | 49.820 | 2.498 | 35 |
| 12 | | | | 0.3 | 0.2 | 0.3 | 49.100 | 2.596 | 27 |

| | | | | | | | | | |
|----|-------|-------------|---------------------------------------|-----|-----|-----|--------|-------|----|
| 13 | 100 % | 66.66 % | $0.6 \times$ $2.4 \times$ 0.6 | 0.1 | 0.2 | 0.1 | 48.926 | 2.568 | 34 |
| 14 | | | | 0.1 | 0.3 | 0.1 | 47.999 | 2.718 | 33 |
| 15 | | | | 0.2 | 0.1 | 0.2 | 50.160 | 2.775 | 37 |
| 16 | | | | 0.2 | 0.3 | 0.2 | 47.878 | 2.777 | 26 |
| 17 | | | | 0.3 | 0.1 | 0.3 | 50.367 | 2.811 | 39 |
| 18 | | | | 0.3 | 0.2 | 0.3 | 47.239 | 2.594 | 26 |
| 19 | 100 % | Fixed layer | | 0.1 | 0.1 | 0.1 | 50.677 | 2.701 | 48 |
| 20 | | | | 0.2 | 0.2 | 0.2 | 48.318 | 2.608 | 27 |
| 21 | | | | 0.3 | 0.3 | 0.3 | 47.978 | 3.058 | 28 |

Table 3. Pareto-optimal set

| S. No | Max. tensile strength (MPa) | Build time (min) | Trade-off |
|-------|-----------------------------|------------------|------------------------------|
| 5 | 49.836 | 31 | The most balanced solution |
| 6 | 49.450 | 26 | The fastest, low-strength |
| 15 | 50.160 | 37 | High strength, slow |
| 17 | 50.367 | 39 | One of the highest strengths |
| 19 | 50.677 | 48 | The slowest, most durable |

Biographies

Vedat Taşdemir studied mechanical engineering at the “Faculty of Technology, University of Fırat, Türkiye”. He is currently working as an associate professor in the Mechanical Engineering Department, Simav Technology Faculty, Kütahya Dumlupınar University. His research areas include additive manufacturing, metal forming, design, and finite element analysis.